



ELSEVIER

Journal of Molecular Catalysis A: Chemical 165 (2001) 103–111

JOURNAL OF
MOLECULAR
CATALYSIS
A: CHEMICAL

www.elsevier.com/locate/molcata

Application of $\{(\text{DMF})_{10}\text{Ln}_2[\text{Pd}(\text{CN})_4]_3\}_\infty$ ($\text{Ln} = \text{Yb}, \text{Sm}$) as lanthanide–palladium catalyst precursors dispersed on sol–gel– TiO_2 in the reduction of NO by methane in the presence of oxygen

A. Rath^a, E. Aceves^b, J. Mitome^b, J. Liu^a, U.S. Ozkan^{b,1}, S.G. Shore^{a,*}^a Department of Chemistry, The Ohio State University, Columbus, OH 43210, USA^b Department of Chemical Engineering, The Ohio State University, Columbus, OH 43210, USA

Received 18 April 2000; accepted 4 September 2000

Abstract

Cyanide bridged lanthanide–palladium transition metal complexes were employed as catalyst precursors in the catalytic reduction of NO with methane. Complexes $\{(\text{DMF})_{10}\text{Ln}_2[\text{Pd}(\text{CN})_4]_3\}_\infty$ ($\text{Ln} = \text{Yb}, \text{Sm}$; DMF = dimethyl formamide) were dispersed (10 wt.% loading based upon palladium) on sol–gel titania supports and reduced by ammonia or hydrogen to metallic nanoparticles containing palladium and lanthanide metals. They were tested for catalytic activity in NO reduction by CH_4 in the presence of oxygen. The bimetallic catalysts were found to be active for NO reduction up to the stoichiometric oxygen concentrations. They displayed improved performance over a palladium only catalyst. Catalysts were examined by TEM, and XPS techniques before, during, and after the reaction. © 2001 Elsevier Science B.V. All rights reserved.

Keywords: Cyanide bridged transition metal complex; Lanthanide–palladium; NO reduction; Methane; Sol–gel

1. Introduction

Li and Armor pioneered the use of lower hydrocarbons for NO_x reduction, specifically CH_4 [1], while Hamada et al. demonstrated reduction in oxygen-rich atmospheres [2,3]. Using a variety of zeolite based catalysts, improvements in NO_x reduction with hydrocarbons has been achieved [4–6]. For example, Li

and Armor have continued their work by investigating NO reduction with methane over Ga–H–ZSM-5 [7] and Co-FER(6) [8] catalysts. Feng and Hall have demonstrated NO reduction with methane using an over-exchanged FeZSM-5 catalyst that is more durable in the presence of steam [9].

In their previous work, Ozkan et al. have shown the use of palladium catalysts in NO reduction with methane [10–12]. They concluded that the oxidation state of palladium was crucial in the NO reduction activity. Using oscillatory behavior of the catalytic system, they have demonstrated that the metallic form of palladium was needed for the NO reduction reaction and the oxide phase of palladium led to

* Corresponding author. Tel.: +1-614-292-6000; fax: +1-614-292-1685.

E-mail addresses: shore@chemistry.ohio-state.edu, ozkan.1@osu.edu (S.G. Shore).

¹ Co-corresponding author. Tel.: +1-614-292-6623.

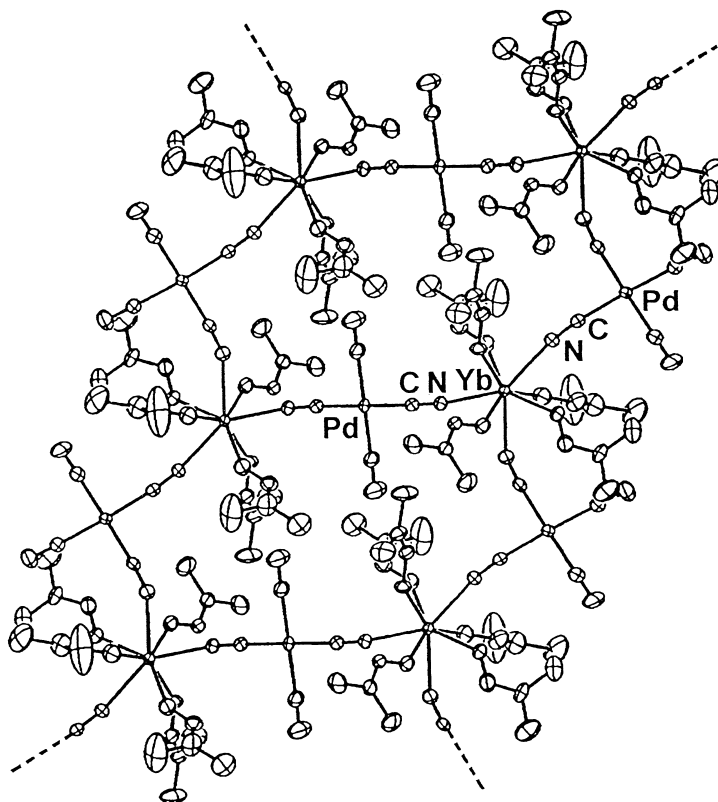


Fig. 1. The molecular structure of the crystalline precursor $\{(\text{DMF})_{10}\text{Yb}_2[\text{Pd}(\text{CN})_4]_3\}_\infty$.

complete combustion of methane. In a later article, they also showed the use of a lanthanide metal in close proximity to the palladium to significantly improve the oxygen tolerance of the catalyst [13]. In the present study, cyanide bridged lanthanide–palladium transition metal complexes were employed as catalyst precursors to bring the lanthanide and the palladium together on an atomic scale. A series of lanthanide transition metal complexes that are extended array structures in the solid state have been prepared in the laboratory of Shore [14]. These structures have regular repeating arrangements of both types of metals that are linked by cyanide bridges. Of particular interest are the isostructural cyanide bridged complexes $\{(\text{DMF})_{10}\text{Ln}_2[\text{Pd}(\text{CN})_4]_3\}_\infty$ ($\text{Ln} = \text{Yb}, \text{Sm}$), (Fig. 1). Such complexes, supported on a surface and reduced to the metallic state, in principle, could provide uniformly dispersed nanoparticles with the dissimilar metals in intimate contact. Such disper-

sions could be effective in heterogeneous catalytic reactions with the transition metal serving as the principal catalyst and the lanthanide functioning as a catalyst promoter. Indeed Imamura et al. showed a synergism with lanthanide promoted palladium catalysts used in hydrogenation reactions [15–17]. However, their procedure is rather involved. In the present study we have examined the application of the complexes $\{(\text{DMF})_{10}\text{Ln}_2[\text{Pd}(\text{CN})_4]_3\}_\infty$ ($\text{Ln} = \text{Yb}, \text{Sm}$; DMF = dimethyl formamide) as precursors for the formation of Yb–Pd and Sm–Pd catalysts on sol–gel titania surface for the purpose of reducing NO by CH_4 in the presence of O_2 . The lanthanide–palladium precursor is relatively easy to prepare [14] and simultaneous impregnation of the support with both metals is easier and simpler than the Imamura method [17]. Therefore, it was of interest to determine if enhanced performance of the palladium catalyst would be promoted by this alternative approach.

2. Experimental

2.1. Sol–gel titania preparation

Excess isopropyl alcohol (~100 ml, Fisher) was used as a solvent for 18.6 ml of titanium(IV) isopropoxide (Aldrich). The alkoxide was added to the solvent while stirring at room temperature. While continuing to stir the solution, 7.9 ml of de-ionized water was added dropwise using a syringe pump at a constant rate. The mixture was allowed to evaporate overnight at room temperature. The dry gel was then calcined under an O₂ stream at 500°C.

2.2. Precursors and bimetallic catalyst preparations

The precursor lanthanide–palladium complexes, $\{(\text{DMF})_{10}\text{Ln}_2[\text{Pd}(\text{CN})_4]_3\}_\infty$ (Ln = Yb, Sm), were prepared and characterized according to a procedure reported in the literature by Shore and co-workers [14]. The sol–gel titania support was impregnated with lanthanide–palladium precursor. The procedure was carried out in a dry box. A weighed amount of precursor complex was added to a weighed amount of sol–gel titania such that the mixture contained 10 wt.% palladium. To this mixture 10 ml of DMF (Mallinckrodt) was added and the resulting suspension stirred for 1–2 h. Typical samples of impregnated sol–gel titania were ones which contained 0.2139 g of $\{(\text{DMF})_{10}\text{Yb}_2[\text{Pd}(\text{CN})_4]_3\}_\infty$ on 0.4000 g sol–gel titania and 0.1979 g of $\{(\text{DMF})_{10}\text{Sm}_2[\text{Pd}(\text{CN})_4]_3\}_\infty$ on 0.3800 g of sol–gel titania. For the experiments that employed only palladium (10 wt.%) on sol–gel titania palladium acetate (Aldrich) was used as the precursor. In a typical experiment 0.0422 g of palladium acetate was combined with 0.200 g of sol–gel titania. DMF was removed under vacuum at room temperature from impregnated sol–gel titania. The resulting white solid was removed in air from its glass container and placed in a quartz boat measuring 3 in. \times 3/8 in. The boat was then placed in a furnace which was flushed with either H₂ or NH₃ for a period of about 10 min, after which time reduction of the impregnated complex was carried out under a steady flow of either ammonia or hydrogen gas (Matheson), with incremental temperature increases of 25°C approximately every 10 min. As the temperature was raised above 200°C, the sample abruptly showed

signs of discoloration. At the final temperature for the ammonia reduction, the sample quickly turned black throughout. When NH₃ gas was the reducing agent, XPS analysis revealed that metals on the titania were completely reduced after 15 min at 275°C. With H₂ complete reduction was achieved in 15 min at 250°C.

A bimetallic catalyst was prepared by separate loading of Pd and Yb on sol–gel titania employing a procedure similar to that of Imamura [17] in order to compare its activity with that of the catalyst obtained from the precursor $\{(\text{DMF})_{10}\text{Yb}_2[\text{Pd}(\text{CN})_4]_3\}_\infty$. A 10 wt.% loading of palladium acetate was weighed, in the glove box, onto the sol–gel titania support. This dispersion was stirred in DMF for one day, then recrystallized under vacuum. The resulting brown powder was reduced under NH₃ at 200°C for 4 h. The reduced material was purposely exposed to the air prior to transfer to a bulb. Approximately 20 ml of dry ammonia was condensed into the flask and kept as a liquid at –40°C. A pre-weighed 10.1 wt.% loading of ytterbium metal shavings were added to the stirred solution from an evacuated arm on the side of the two-necked flask. The ytterbium metal turned the solution blue after five minutes of stirring. After 20 min, the blue color faded to gray-brown. Yet after another 20 min, the solution became pale blue in color. The ammonia was pumped away from the system, initially at –40°C and when there was apparently no more ammonia in the system, the system was pumped on at room temperature for 4 h.

2.3. Characterization

Single crystal X-ray structures and IR spectra of the $\{(\text{DMF})_{10}\text{Ln}_2[\text{Pd}(\text{CN})_4]_3\}_\infty$ (Ln = Yb, Sm) were reported previously [14]. Fully reduced samples prepared for X-ray photoelectron spectroscopy (XPS) analysis were handled in an argon glove box. The XPS spectra were obtained with an X-ray source of Mg K α radiation (1253.6 eV) on a Physical Electronics/Perkin-Elmer model 550 ESCA/Auger instrument. The C 1s binding energy, typically 284.6 eV, was used as the charge correction reference for the supported catalysts. Transmission electron microscopy images were obtained with a Philips CM300 TEM using a 1 k \times 1 k CCD camera. The CM300 TEM operates at 300 kV and can provide up to 1.7 Å point-to-point resolution. Elemental analysis was

done on the TEM with an EDAX ultra-thin window energy dispersive X-ray (EDX) detector. The beam was focused to a fine probe for the elemental analyses. A Micromeritics 2100E Accusorb instrument was used for BET surface area analysis.

2.4. Reaction studies

The NO reduction studies were carried out in a fixed-bed flow reactor. The Pd content in the reactor was maintained constant for each reaction. The total flow rate of the feed stream was maintained at 61.5 ml (STP)/min. The NO concentration was fixed at 1780 ppm and the methane at 2.13%. The in situ hydrogen reduction of the precursors was performed using 33% H₂ concentration, with the balance helium. The reduction step was continued for 30 min at 200°C. The flow reactor was subsequently flushed with helium for a minimum of 45 min before the temperature was increased to 500°C for the catalytic reaction experiment.

The product gas analysis was performed using on-line NO_x and NH₃ analyzers and a gas chromatograph. Nitric oxide in the product flow was measured by a chemiluminescence NO–NO_x analyzer from Thermo Environmental Instruments, model 42H. In turn, the ammonia formation was detected and quantified by a Siemens Ultramat 5F IR ammonia analyzer. A Hewlett Packard 5890A on-line gas chromatograph was used to quantify N₂, N₂O, CO, CO₂, O₂, and CH₄ concentrations. This GC is equipped with a 10 ft × 1/8 in. Porapaq Q column and an 8 ft × 1/8 in. molecular sieve column connected in series through a column–isolation valve system.

3. Results

3.1. Catalyst preparation and characterization of precursors and fresh catalysts

The catalysts used in this study were derived from $\{(\text{DMF})_{10}\text{Ln}_2[\text{Pd}(\text{CN})_4]_3\}_\infty$ (Ln = Yb, Sm) precursors which provide a two lanthanide to three palladium metal atom ratio on the support surface. Surface areas of freshly prepared catalysts were in the range 31–39 m²/g, while the surface area of freshly prepared sol–gel TiO₂ was of the order of 80 m²/g.

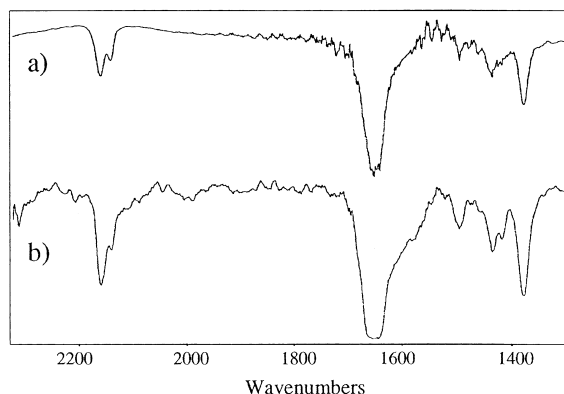


Fig. 2. IR spectra (KBr pellet) of precursor $\{(\text{DMF})_{10}\text{Yb}_2[\text{Pd}(\text{CN})_4]_3\}_\infty$: (a) pure crystalline precursor; (b) precursor dispersed on sol–gel titania.

Infrared spectra of bulk precursors $\{(\text{DMF})_{10}\text{Ln}_2[\text{Pd}(\text{CN})_4]_3\}_\infty$ (Ln = Yb, Sm) and infrared spectra of the precursors supported on titania are presented in Fig. 2. They show that within the resolution of the spectrometer (2 cm^{−1}) there is no difference between the two spectra in the cyanide stretching region which consists of a terminal CN stretch at 2159 cm^{−1} and a bridge CN stretch at 2141 cm^{−1}. This result, in particular the presence of CN bridges, plus the general similarity of the two spectra suggests that the impregnated precursor complex retains the structural feature of Ln–CN–Pd links that is present in the bulk complex.

3.2. Catalyst performance

Catalysts prepared by the above described technique bringing a lanthanide element in intimate contact with the Pd metal over sol–gel titania support were compared to those that contained only palladium in catalytic reduction of NO by methane in the presence of varying concentrations of oxygen. The reaction temperature was fixed at 500°C for all sets of experiments. The NO and CH₄ concentrations were kept constant at 1780 ppm and 2.13%, respectively. The oxygen concentration was varied in the range of 2.00–4.30%.

The NO conversion, N₂ and CO₂ selectivities are presented in Table 1. Catalysts prepared by reduction with ammonia and reduction with hydrogen showed no significant difference in activity. At lower oxygen concentrations all three catalysts, Pd/Yb, Pd/Sm and

Table 1
Results of catalytic NO reduction by supported bimetallic catalysts in a NO + CH₄ + O₂ feed stream

Catalyst	O ₂ concentration			
	3.00%	3.50%	4.00%	4.26%
NO conversion				
10 wt.% 3Pd–2Yb	99.9	99.8	99.9	74.3
10 wt.% 3Pd–2Sm	NA	99.9	99.9	39.6
10 wt.% Pd-only	99.9	99.9	99.9	0
N ₂ selectivity				
10 wt.% 3Pd–2Yb	71	83	93	98
10 wt.% 3Pd–2Sm	NA	78	88	97
10 wt.% Pd-only	78	83	92	0
CO ₂ selectivity				
10 wt.% 3Pd–2Yb	88	94	98	100
10 wt.% 3Pd–2Sm	NA	100	100	100
10 wt.% Pd-only	100	100	100	100

Pd only, can reduce NO essentially completely. Another feature to note, Table 1, is that at lower oxygen concentrations, there are significant levels of ammonia formation. The nitrogen selectivity increases with increasing oxygen concentration, approaching >97% at O₂ concentrations of 4.00% and above. It is also seen that CO selectivity decreases rapidly with increasing O₂ concentrations.

The difference between the lanthanide-promoted catalysts and Pd-only catalysts becomes clearer at higher oxygen concentrations. While all three catalysts perform equally well at oxygen concentrations of 4% or lower, lanthanide-containing catalysts are seen to maintain their activity at higher oxygen concentration levels. At an oxygen concentration of 4.26%, the Yb and Sm containing catalysts are seen to have significant activity while the Pd-only catalyst is completely inactive. This oxygen concentration is significant, since it represents the stoichiometric oxygen concentration for the methane inlet. The Yb-containing catalyst continues to give NO conversion levels close to 70% even above the stoichiometric oxygen concentrations.

For each catalyst that lost its activity, standard regeneration procedures were applied. The regeneration involves re-reducing the catalysts in situ using 33% H₂ in He at 200°C for 0.5 h. All of the regenerated catalysts were able to recover their pre-deactivation activity. This observation is consistent with the earlier

conclusions that the metallic Pd provides the active sites for NO reduction with CH₄ while PdO is mainly responsible for the methane combustion reaction [12].

As mentioned in the Introduction, the work of Imamura et al. relates to dispersing lanthanides dissolved in liquid ammonia on catalysts [15–17]. The Yb–Pd catalyst on sol–gel titania we prepared in a procedure similar to that of Imamura was evaluated. The catalyst showed 99% NO conversion at 3.5% oxygen, but deactivated at 4% oxygen.

3.3. Pre- and post-reaction characterization of the catalysts

Pre- and post-reaction characterization of the catalysts were performed using X-ray photoelectron spectroscopy. Following reduction or reaction, catalysts were transferred to the XPS chamber without being exposed to air using a controlled-atmosphere. Table 2 summarizes the XPS results for the freshly reduced catalysts, the catalysts operating with 4.00% oxygen in the feed stream, and a deactivated 2Yb–3Pd sample.

Following the initial reduction with ammonia at 275°C, the 10 wt.% 2Yb–3Pd catalyst contained palladium in a reduced state of 334.3 eV (Table 2). The palladium in the freshly reduced 10 wt.% 2Sm–3Pd catalyst had a binding energy of 334.1 eV. These XPS values match the expected oxidation state (334.1 eV) for sol–gel titania catalyst systems in which the palladium is Pd(0). While successfully reducing NO at 4.00% oxygen in the feed stream, the 2Yb–3Pd

Table 2
XPS results from (2Ln–3Pd)-bimetallic catalysts on sol–gel TiO₂

10 wt.% 2Yb–3Pd	Metal/shell	XPS value (eV)	Pd ⁰ (%)	PdO (%)
Reduced	Pd 3d5 Yb 4d5	334.2 184.5	100	0
Operational	Pd 3d5 Yb 4d5	335.1/336.2 184.5	40	60
Deactivated	Pd 3d5 Yb 4d5	335.7 184.5	0	100
Reduced	Pd 3d5 Sm 3d5	334.1 1082.9	100	0
Operational	Pd 3d5 Sm 3d5	334.9/335.8 1082.0	?	?

and 2Sm–3Pd catalysts were sealed and the oxidation states assessed again. The palladium in both the 2Yb–3Pd and the 2Sm–3Pd catalysts existed as Pd(0) and Pd(II)O states. When the 2Yb–3Pd catalyst was exposed to oxygen concentrations above 4.30% oxygen, the catalyst was steadily and completely deactivated over the course of 1/2 h. The XPS analysis of the deactivated 2Yb–3Pd catalyst contained palladium exclusively in the fully oxidized state, 335.7 eV.

The oxidation state of the ytterbium metal in the 10 wt.% catalysts remained essentially constant at 184.5 eV for the reduced, operational, and deactivated trials. There may be two ytterbium oxidation states present based on the difference observed in the spectra of the freshly reduced catalyst and the operational catalyst. The peaks at 184.5 eV observed over the operational and deactivated ytterbium catalysts showed

possible slight splitting. Unfortunately, these features were undistinguishable from noise, using deconvolution software. XPS data showed that the samarium in the 10 wt.% 2Sm–3Pd catalyst was at 1082.9 eV when freshly reduced. After operation with 4.00% oxygen present, the oxidation state of samarium was found to be 1082.0 eV. It is unclear whether the samarium metal was undergoing reduction during the operation of the catalyst, or if the sample's surface charging was corrected slightly differently. The reduced and operational 2Sm–3Pd catalyst XPS spectra showed no distinguishable splitting of the oxidation states.

TEM analyses of the catalysts on sol–gel titania supports were obtained before and after catalytic runs. Fig. 3 is a TEM micrograph of a freshly reduced Yb–Pd catalyst on sol–gel titania support obtained by reducing $\{(\text{DMF})_{10}\text{Yb}_2[\text{Pd}(\text{CN})_4]_3\}_\infty$ (10 wt.% Pd)

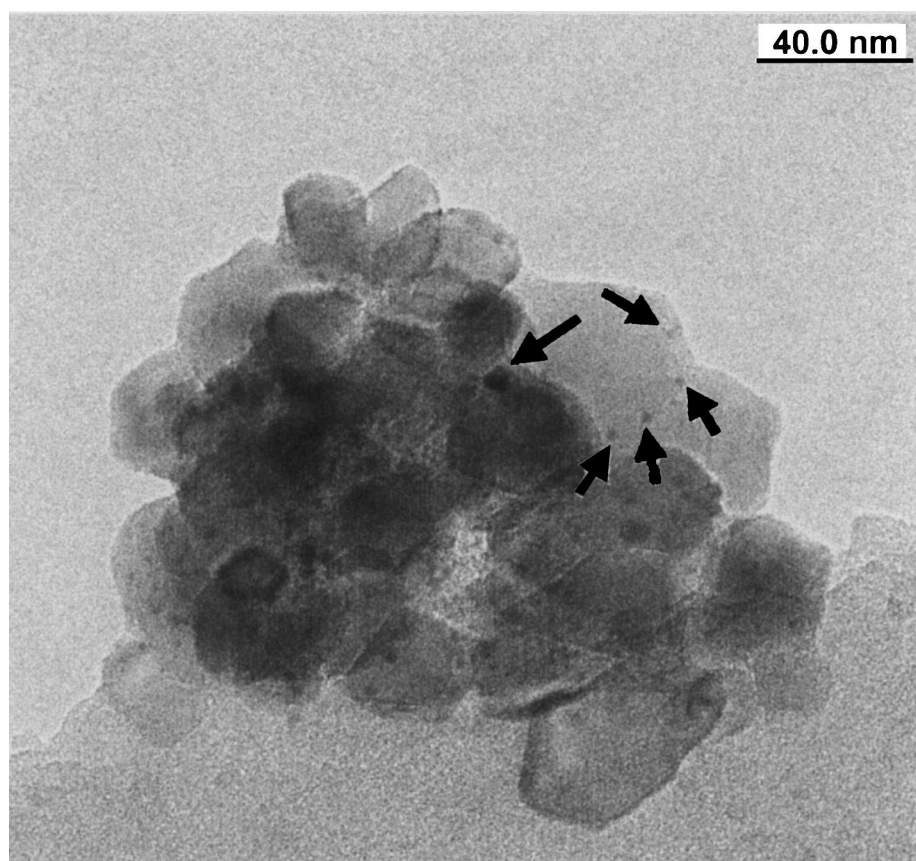


Fig. 3. TEM of freshly reduced 10 wt.% 3Pd–2Yb on sol–gel titania. The arrows point to a 10 nm particle with Pd to Yb ratio of 3:1 and regularly spaced 3 nm bimetallic particles with Pd to Yb ratios of 1:1 to the right of the 10 nm particle.

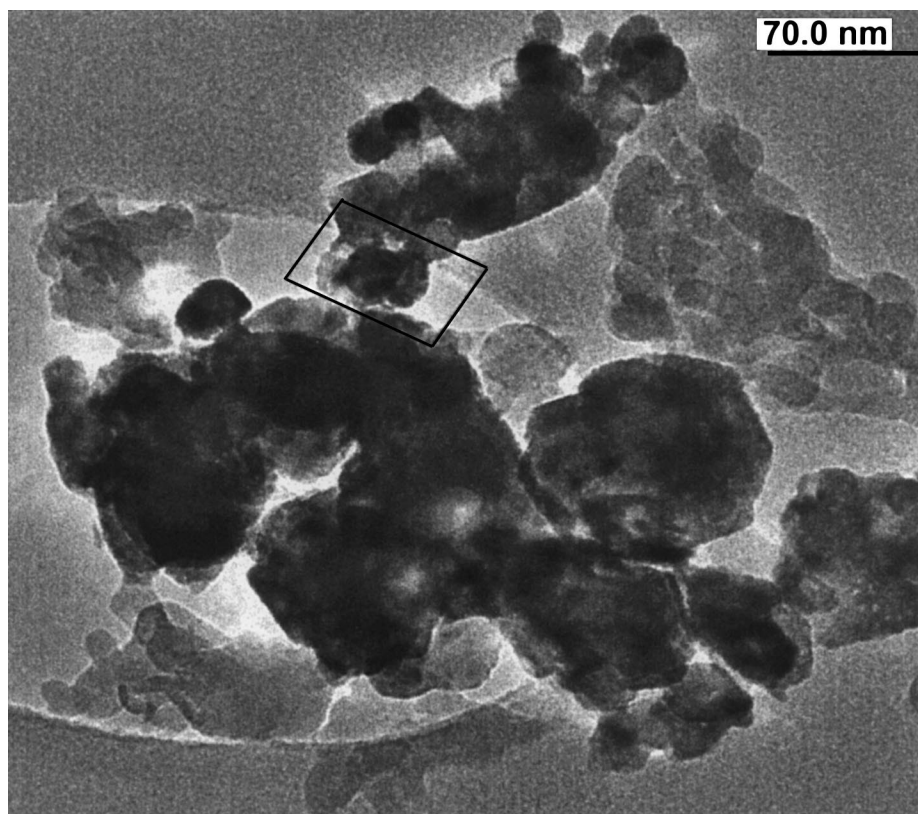


Fig. 4. TEM of 10 wt.% 3Pd–2Yb on sol–gel titania after reduction of NO with 4.00% oxygen in the feed stream (18 h).

with NH_3 at 250°C . The arrow points to a 10 nm particle with the Pd to Yb ratio of 3:1. Palladium and ytterbium can form an alloy of the formula Yb_3Pd_4 [18]. Regularly spaced 3 nm bimetallic particles were observed on the shelf edge, just to the right of the 10 nm particle. Energy dispersive X-ray analysis indicated that these particles have approximately 1:1 metal ratios.

A TEM micrograph of a post-reaction sample of the same batch of catalyst is shown in Fig. 4. This sample had successfully functioned in a feed stream of 4.00% oxygen, 2.13% methane, and 1780 ppm nitric oxide at 500°C for 8 h. The morphology of the boxed region in Fig. 4 is enlarged in Fig. 5. In the center of Fig. 5 is a large, dark 35 nm particle surrounded by a lighter ‘skirt’ region. EDX determined that the central particle had a palladium to ytterbium ratio of 10:1. Meanwhile, the skirt surrounding the dark particle has a much higher ytterbium content, approximately 1:6;

Pd:Yb. The faint, light colored holes in the center of the palladium particle were created in the process of EDX focusing (300 kV). Comparison of this photograph with that in Fig. 3 reveals that at 500°C under the conditions of catalysis, the palladium accumulated into larger agglomerates. The small bimetallic particles present in Fig. 4 were not observed in Fig. 5. However, the larger Pd particle remained in contact with a ring of metal rich in Yb.

4. Discussion

The precursor lanthanide–palladium complexes, $\{(\text{DMF})_{10}\text{Ln}_2[\text{Pd}(\text{CN})_4]_3\}_\infty$ ($\text{Ln} = \text{Yb}, \text{Sm}$), which allow Yb or Sm metal and Pd metal to be in intimate contact at atomic level, were prepared and dispersed onto a titania support prepared by the sol–gel method. The IR spectra confirmed that the structural features

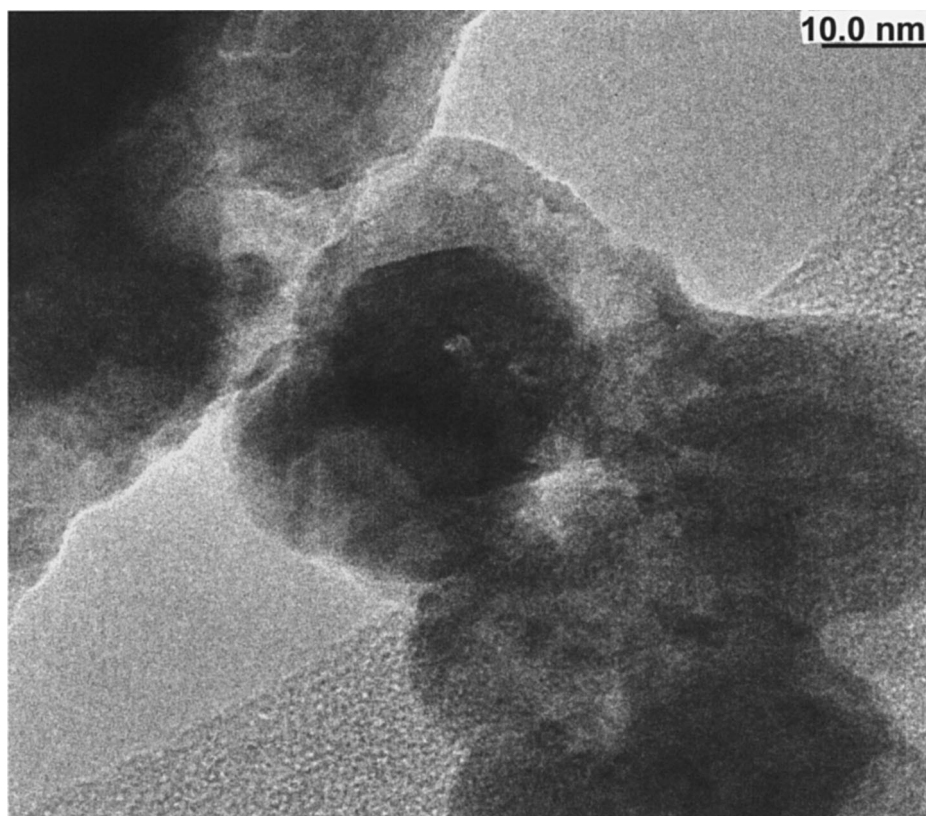


Fig. 5. Enlarged rectangular region from Fig. 4. The dark cluster in the center has a Pd:Yb ratio of 6:1 (faint white spots in the middle of the Pd cluster are EDX “burns”). Faint shaded region surrounding the cluster is predominantly Yb in content.

of Ln–CN–Pd links of the precursor complex were retained even after they were dispersed on to the support.

Sol–gel titania was selected because of its ability to disperse particles of a bimetallic nature. After reduction, bimetallic particles on sol–gel TiO_2 showed little tendency to sinter. The bimetallic catalysts supported on sol–gel titania showed high activity and selectivity for reduction of NO to N_2 . When compared to the Pd-only catalyst with the same loading level, the bi-metallic catalyst had a significantly higher oxygen tolerance. The Pd XPS spectra of post-reaction of active bimetallic catalysts showed both metallic and oxidized states of Pd co-existing on the surface. Since the Pd XPS spectrum of deactivated Yb–Pd bimetallic catalyst showed complete oxidation, it is concluded that the active phase of the catalysts is the Pd(0) state. The results are consistent with those previously reported

[10–13]. These results suggest that the intimate contact of lanthanide element and Pd helps Pd to be in the metallic phase under more oxidizing conditions than Pd alone. It is conceivable that the use of a strongly electropositive lanthanide metal in close contact with the Pd can inhibit the oxidation of the precious metal.

Another interesting feature of these catalysts was their increasing selectivity toward N_2 and CO_2 as the O_2 concentration in the feed was raised. One explanation toward the improvement of N_2 selectivity could be due to oxidation of ammonia that was produced as a side product of $\text{NO} + \text{CH}_4 + \text{O}_2$ reaction. The increase in CO_2 selectivity could be simply due to CO in the reactor that was driven to further react with O_2 to produce CO_2 .

The initial goal, to form intimate bimetallic particles, was achieved following the reduction of the lanthanide-transition metal precursor with ammonia at

275°C. After use of the catalysts at 500°C, the originally bimetallic nature of the particles partially gave way to phase separated agglomerates. However, catalytic activity did not diminish until the O₂ concentration reached above-stoichiometric levels suggesting that the redistribution of the metals may not be critical as long as intimate contact is maintained between the two metals.

5. Conclusions

Application of lanthanide–palladium catalysts toward NO reduction in the presence of oxygen has demonstrated improved performance over a palladium-only catalyst. The novel selection of a $\{(\text{DMF})_{10}\text{Ln}_2[\text{Pd}(\text{CN})_4]_3\}_\infty$ (Ln = Yb, Sm), precursor enabled a uniform ratio of metals to be delivered in an intimate fashion and was simpler and easier to carry out than the more conventional technique of separate impregnation of the two metals on the support surface. Furthermore, the catalysts obtained from $\{(\text{DMF})_{10}\text{Ln}_2[\text{Pd}(\text{CN})_4]_3\}_\infty$ (Ln = Yb, Sm), are more effective than the example studied in the present investigation, that was prepared by separate impregnation of the two metals.

Acknowledgements

Support to S.G.S. by the National Science Foundation through Grants CHE 99-0115 and CHE 97-00394

and support to U.S.O. by the National Science Foundation through Grant CTS-9412544 and from Ohio Coal Development Office are gratefully acknowledged.

References

- [1] Y. Li, Y.N. Armor, Appl. Catal. B 3 (1993) L1.
- [2] H. Hamada, Y. Kintaichi, M. Sasaki, T. Ito, Appl. Catal. 64 (1990) L1.
- [3] H. Hamada, Y. Kintaichi, M. Sasaki, T. Ito, Appl. Catal. 75 (1990) L1.
- [4] Y. Ukisu, S. Sato, A. Abe, K. Yoshida, Appl. Catal. B 2 (1993) 147.
- [5] K.A. Bethke, C. Li, M.C. Kung, B. Yang, H.H. Kung, Catal. Lett. 31 (1995) 287.
- [6] J.S. Feeley, M. Deeba, R.J. Farrauto, G. Beri, A. Haynes, Appl. Catal. B 6 (1995) 79.
- [7] Y. Li, J.N. Armor, J. Catal. 145 (1994) 1.
- [8] Y. Li, J.N. Armor, J. Catal. 150 (1994) 376.
- [9] X. Feng, W.K. Hall, J. Catal. 166 (1997) 368.
- [10] M.W. Kumthekar, U.S. Ozkan, J. Catal. 171 (1997) 45.
- [11] M.W. Kumthekar, U.S. Ozkan, J. Catal. 171 (1997) 54.
- [12] U.S. Ozkan, M.W. Kumthekar, G. Karakas, J. Catal. 171 (1997) 67.
- [13] J. Mitome, E. Aceves, U.S. Ozkan, Catal. Today 53 (1999) 597.
- [14] D.W. Knoepfel, J. Liu, E.A. Meyers, S.G. Shore, Inorg. Chem. 37 (1998) 4828.
- [15] H. Imamura, Y. Miura, K. Fujita, Y. Sakata, S. Tsuchiya, J. Mol. Catal. A 140 (1999) 81.
- [16] H. Imamura, K. Igawa, Y. Sakata, S. Tsuchiya, Bull. Chem. Soc. Jpn. 69 (1996) 325.
- [17] H. Imamura, K. Igawa, Y. Kasuga, Y. Sakata, S. Tsuchiya, J. Chem. Soc., Faraday Trans. 90 (1994) 2119.
- [18] A. Palenzona, A. Iandelli, J. Less Commun. Met. 34 (1974) 121.